

THE COMPOUNDING EFFECTS OF TROPICAL DEFORESTATION AND GREENHOUSE WARMING ON CLIMATE

H. ZHANG^{1*}, A. HENDERSON-SELLERS² and K. MCGUFFIE³

¹*Bureau of Meteorology Research Centre, Melbourne, Australia*

²*Environment Division, Australian Nuclear Science and Technology Organisation, Sydney, Australia*

³*Department of Applied Physics, University of Technology, Sydney, Australia*

Abstract. This study reports the first assessment of the compounding effects of land-use change and greenhouse gas warming effects on our understanding of projections of future climate. An AGCM simulation of the potential impacts of tropical deforestation and greenhouse warming on climate, employing a version of NCAR Community Climate Model (CCM1-Oz), is presented. The joint impacts of tropical deforestation and greenhouse warming are assessed by an experiment in which removal of tropical rainforests is imposed into a greenhouse-warmed climate. Results show that the joint climate changes over tropical rainforest regions comprise large reductions in surface evapotranspiration (by about -180 mm yr^{-1}) and precipitation (by about -312 mm yr^{-1}) over the Amazon Basin, along with an increase of surface temperature by $+3.0 \text{ K}$. Over Southeast Asia, similar but weaker changes are found in this study. Precipitation is decreased by -172 mm yr^{-1} , together with the surface warming of 2.1 K . Over tropical Africa, changes in regional climate is much weaker and with some different features, such as the increase of precipitation by 25 mm yr^{-1} . Energy budget analyses demonstrates that the large increase of surface temperature in the joint experiment is not solely produced by the increase of CO_2 concentration, but is a joint effect of the reduction of surface evaporation (due to deforestation) and the increase of downward atmospheric longwave radiation (due to the doubling of CO_2 concentration). Furthermore, impacts of tropical deforestation on the greenhouse-warmed climate are estimated by comparing a pair of tropical deforestation simulations. It is found that in CCM1-Oz, deforestation has very similar impacts on greenhouse-warmed regional climates as on current climates over tropical rainforest regions. The extra-tropical climatic response to tropical deforestation is identified in both sets of tropical deforestation experiments. Statistically significant responses are seen in the large-scale atmospheric circulation such as changes in the velocity potential and vertically integrated kinetic and potential energy fields. Wave propagation patterns are identified in the large-scale circulation anomalies, which provides a mechanism for interpreting the model responses in the extra-tropics. In addition, this study suggests that land-use change such as tropical deforestation may affect projections of future climate.

1. Introduction

Many published Global Climate Model (GCM) simulations have shown that tropical deforestation may affect regional and even large-scale climate in the tropics (e.g., Zhang et al., 1996a,b; Sud et al., 1996). Results have further indicated that impacts of tropical deforestation depend upon regional climate characteristics in

* Corresponding address: BMRC, GPO Box 1289k, VIC 3001, Australia.
E-mail: h.zhang@bom.gov.au



Climatic Change **49**: 309–338, 2001.

© 2001 Kluwer Academic Publishers. Printed in the Netherlands.

the tropics where disturbances are imposed (e.g., Mylne and Rowntree, 1992; Henderson-Sellers et al., 1993; Polcher and Laval, 1994; Zhang et al., 1996a,b). Therefore, it is of scientific value to assess how the impacts of tropical deforestation differ in warmed climate from that in the current climate. Tropical deforestation is known to be contributing to the increasing atmospheric carbon dioxide burden and hence the warming of climate (e.g., Houghton et al., 1990, 1992, 1996). Despite these acknowledged compounding effects of tropical deforestation and greenhouse warming, there are, as yet, very few published papers exploring the possible impacts of tropical deforestation in a greenhouse-warmed climate, or assessing the joint regional effects of greenhouse warming and tropical deforestation.

This paper aims to report a preliminary assessment by means of a pair of experiments in which a doubling of atmospheric CO₂ concentration and the removal of tropical rainforest are imposed individually and in combination, in a similar fashion used by Henderson-Sellers et al. (1995) for the study of stomatal resistance. Despite the fact that the model used in this study has been substantially revised and improved since these experiments were conducted, we believe that scientific results derived from the experiments are still of value in understanding how tropical deforestation may affect future climate. In addition, this pair of experiments provides the first evaluation of how land use change in the tropics may compound uncertainties in our projections of future climate. The combined imposition of tropical deforestation and greenhouse warming can be viewed as the worst (but also the most likely) case scenario for tropical rainforest regions. By comparing results from the joint experiment with the separately imposed CO₂ doubling and tropical deforestation impacts, it is anticipated that the joint impacts of deforestation and greenhouse warming can be more effectively assessed.

The experiments used in this study are described in Section 2. Four simulations using a version of National Center for Atmospheric Research (NCAR) Community Climate Model (CCM1-Oz) were conducted. Section 3 describes the joint effects of tropical deforestation and doubling of the atmospheric CO₂ concentration on the regional and global climate. In Section 4, impacts of tropical deforestation in a greenhouse-warmed climate are assessed by comparing the joint effect in Section 2 with the results from the doubling of CO₂ concentration alone. The compounding effects of greenhouse warming and tropical deforestation are studied by comparing the joint effects with the deforestation alone results. In Section 5, we revisit the hypothesis that large-scale tropical deforestation could induce extra-tropic climate disturbances. In addition, the issue of how land-use may affect our projection of future climate is discussed. Finally, conclusions and discussions from this study are presented in Section 6.

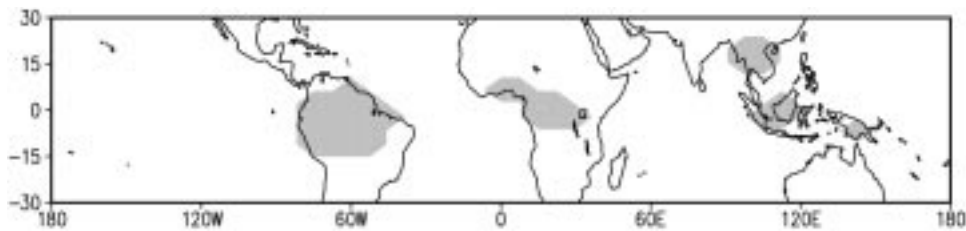


Figure 1. Locations of three deforestation regions used in this study. Shaded areas are the deforested grid-cells in the model R15 resolution.

2. Experimental Simulations Assessed

All the experiments analyzed in this study were conducted using CCM1-Oz. These results complete a set of published papers on the impacts of tropical deforestation (e.g., McGuffie et al., 1995; Henderson-Sellers et al., 1995; Zhang et al., 1996a,b). In this model (a modified version of NCAR CCM1 with R15 spectral truncation) a full diurnal cycle was included to permit adequate simulation of land surface characteristics. The energy balance at the top of the atmosphere throughout the diurnal cycle was ensured by tuning the cloud liquid water parameterizations (Slingo, 1989). A mixed-layer slab-ocean of 50 m depth with q-flux correction and a three-layer sea-ice sub-model was used as the model's ocean component. The Biosphere-Atmosphere Transfer Scheme (BATS1e) (Dickinson et al., 1993) was incorporated in CCM1-Oz to capture the importance of land-surface processes in regional and global climate.

Four CCM1-Oz experiments are analyzed in this study to assess the joint effects of tropical deforestation and greenhouse warming. Results presented in this study are derived from (1) a 25-year control experiment; (2) an 11-year tropical deforestation experiment over the Amazon Basin, Southeast Asia and tropical Africa as shown in Figure 1 (the same as used in Zhang et al., 1996a,b); (3) a 10-year doubled- CO_2 concentration simulation after the CO_2 concentration was instantaneously increased from 330 ppmv to 660 ppmv globally and after the time when the model climate had equilibrated (hereafter called the $2 \times \text{CO}_2$ experiment); and (4) a 10-year tropical deforestation in a doubled atmospheric CO_2 concentration environment in which the same tropical rainforests were removed but in the equilibrated doubled CO_2 climate (hereafter called the joint experiment).

The 'deforestation' was imposed in the same way as in the previous similar experiments (e.g., McGuffie et al., 1995) i.e., by replacing forests with grassland and modifying soil characteristics. This leads to increase in the surface albedo, reduction in the surface roughness, reduction in the leaf area index (LAI), soil colour brighter and texture coarser. In the deforestation experiments reported here, surface roughness is reduced from 2.0 m to 0.2 m, surface albedo increased from 12% to 19%, minimum leaf area index decreased from 5.0 to 0.5, and soil colour

brightened by two classes. Details of other changes are the same as Henderson-Sellers et al. (1993).

By comparing results from the joint experiment and the control experiment, climate changes due to doubling the CO₂ concentration and deforesting all the tropical rainforest regions can be assessed. These impacts can then be evaluated in three ways. Firstly, the differences between the joint experiment and the 2×CO₂ experiment represent the impacts of tropical deforestation in a greenhouse-warmed climate. Secondly, comparing the impacts of tropical deforestation under the greenhouse-warmed climate with those of deforestation under present-day climate (cf. Zhang et al., 1996a,b) allows consideration of the question of whether the climatic impacts due to tropical deforestation are enhanced or dampened by greenhouse warming. Thirdly, comparing results of model-simulated impacts of deforestation with the model-simulated climate change due to the enhanced CO₂ concentration allows us to assess how land use change may alter our prediction of future climate.

It is essential to note that these four experiments offer only a preliminary view of the potential combined effects of greenhouse warming and tropical deforestation. There are a number of significant features which have been omitted in these experiments. These include: (i) the effect of CO₂ fertilization of plant growth; (ii) the effect on canopy conductance caused by CO₂ increase which may provide a significant climatic forcing in a CO₂-enriched atmosphere (Henderson-Sellers et al., 1995; Sellers et al., 1996; Cox et al., 1999); (iii) possible changes in ocean circulation patterns which cannot be captured by the mixed-layer model used here; and, similarly, (iv) possible changes in the monsoon circulation and ENSO patterns, among other things, which depend upon adequate simulations of the ocean uptake of heat (cf. Meehl and Washington, 1993, 1996).

3. Joint Climatic Changes Due to Doubling the CO₂ Concentration and Tropical Deforestation

The major goal of this section is to display and describe the combined climatic impacts of doubling the atmospheric CO₂ concentration and tropical deforestation over the three major tropical rainforest regions of the globe: the Amazon Basin, Southeast Asia and tropical Africa. These are assessed in terms of the differences between the joint experiment and the control experiment. In addition, possible physical connections between greenhouse warming and tropical deforestation are studied by analyzing changes in surface and atmospheric energy budgets as well as the changes in water vapour transport.

Prior to studying the model-simulated climatic changes following deforestation and greenhouse warming, the control simulation of current climate over tropical rainforest regions as well as a range of global features have been evaluated, as shown in detail by McGuffie et al. (1995). Despite the fact that the model was

formulated with a low resolution (R15, roughly 4.5° latitude by 7.5° longitude), the main climatic features over tropical rainforest regions, such as the rainfall and surface temperature spatial patterns and seasonal variations, are reasonably well reproduced. In the rest of the paper, regional and global climate changes following deforestation and greenhouse warming are referred to the basic state derived from the model's 25-year control simulation (cf. McGuffie et al., 1995). If the results presented here are deemed interesting they may prompt repeat experiments using higher resolution models and/or improved physical parameterisations which recent studies suggest may lead to a better control simulations over the tropical forest regions (e.g., Hahmann and Dickinson, 1997).

3.1. ANNUALLY AVERAGED JOINT IMPACTS OVER TROPICAL RAINFOREST REGIONS

Table I shows the model-simulated surface climate in the annually averaged control, deforestation, $2 \times \text{CO}_2$, and joint experiments over three tropical rainforest regions. Results are the averages of the 25-year control experiment, 11-year deforestation experiment, and 10-year $2 \times \text{CO}_2$ and joint experiments. The differences between area-averaged climate in the joint experiment and control experiment represent the regional climate impacts due to tropical deforestation and doubling the atmospheric CO_2 concentration.

Over the Amazon Basin, a large reduction in surface evapotranspiration ($-14.9 \text{ mm month}^{-1}$) is seen in the joint as compared to the control experiment. This decrease can, to a large extent, be explained as being due to the reduction in the effective evaporation area and in the surface roughness length. The reduction in surface roughness decouples the mixing processes between the land-surface and the low-level atmosphere and the reduction of vegetation leaf area index causes the decrease in vegetation interception of precipitation (cf. Zhang et al., 1996a) and transpiration. A drier climate is simulated where total precipitation decreases by $-26.4 \text{ mm month}^{-1}$ following deforestation and doubling the CO_2 conditions. As found in Zhang et al. (1996a), there are two factors which responsible for the decrease of precipitation over the Amazon Basin. One is the weakened local water recycling in the forest basin (i.e., the decrease in surface evaporation moistening the overlying atmosphere). The other is associated with the change of regional atmospheric circulation. Calculation of vertical integrated water vapour transport, which will be discussed later (cf. Figure 3), suggests that the water vapour transport into the basin is reduced (cf. Zhang, 1995), associated with a weakening of low-level atmospheric convergence.

In the surface energy balance (cf. Figure 2a), net incident solar radiation at the surface is decreased by -6.1 W m^{-2} primarily due to the increase of surface albedo. On the other hand, deforestation leads to a large reduction in surface latent heat (-12.2 W m^{-2}). Thus the net effect is that the deforested surface gains extra energy of $+6.1 \text{ W m}^{-2}$. This extra component of energy is then used to heat the land-

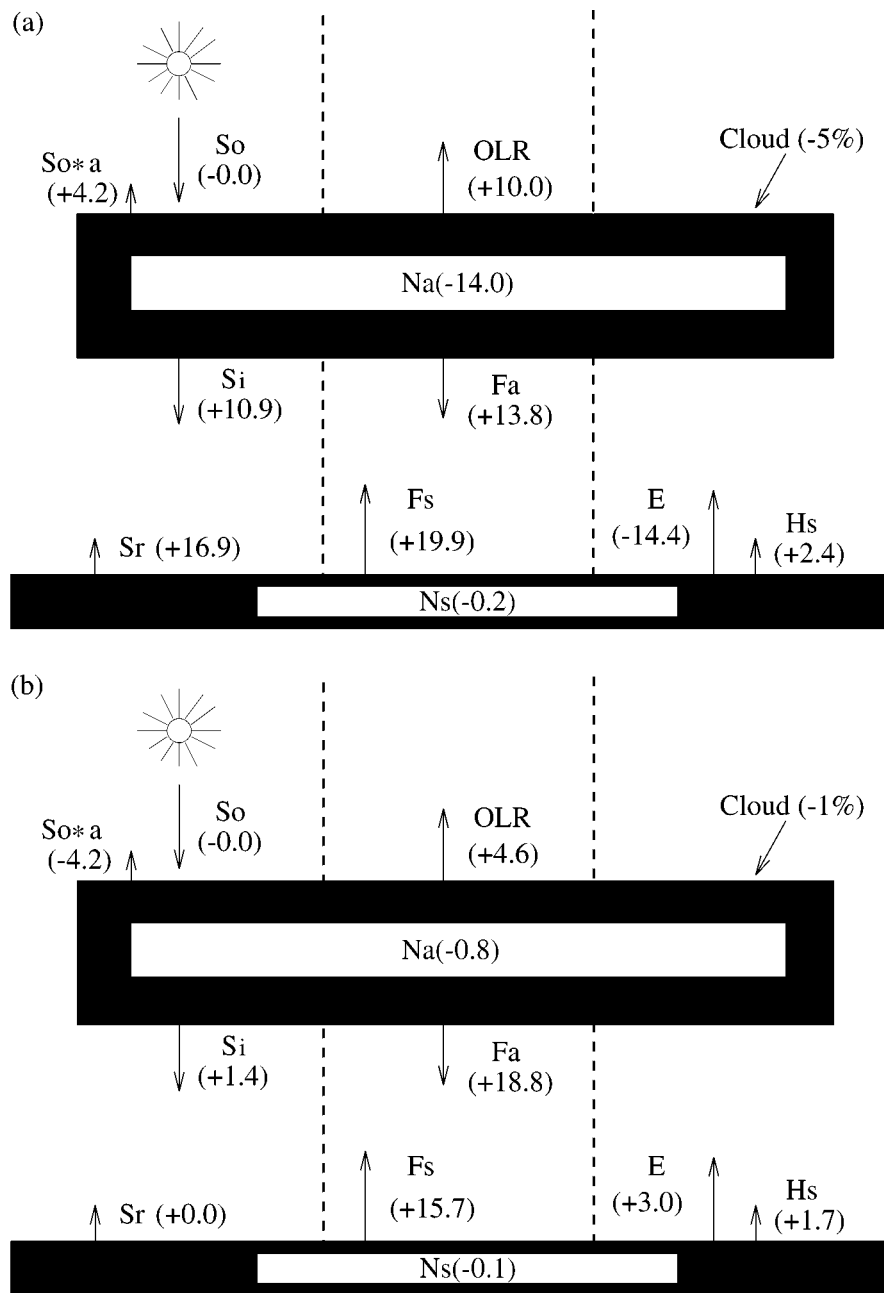


Figure 2. Areal averaged annual changes in the surface and atmospheric energy budgets over the deforestation grid points in the Amazon Basin as shown in Figure 1. (a) Differences over the Amazon Basin between joint and control experiments; (b) Differences over the Amazon Basin between $2 \times CO_2$ and control experiments. S_o is the incident solar radiation at the top of the atmosphere; OLR is the outgoing longwave radiation at the top of the atmosphere; $Cloud$ represents the total cloudiness; N_a is the net atmospheric energy budget; S_i is the incident solar radiation reaching the surface; F_a is the downward longwave radiation reaching the surface; S_r is the solar radiation reflected by the surface; F_s is the longwave radiation from the surface; E is the surface latent heat flux; H_s is the surface sensible heat flux and N_s is the residual of surface energy balance. All the variables except $Cloud$ have the same unit as $W m^{-2}$.

TABLE I

Annually-averaged changes in the surface climate over the tropical rainforest regions in the CCM1-Oz control simulation (Ctl); deforestation simulation (Def); $2 \times \text{CO}_2$ simulation ($2 \times \text{CO}_2$); and joint experiment. T_s is the surface air temperature (K); P the monthly total precipitation (mm month^{-1}); P_c the convective precipitation (mm month^{-1}); R the surface net radiation (W m^{-2}); E the surface evapotranspiration (mm month^{-1}) and H_s the surface sensible heat flux (W m^{-2}). Results are the land areal averages over the regions shown in Figure 1

		T_s	P	P_c	R	E	H_s
Amazon	Ctl.	298.69	158.19	97.08	156.42	103.58	56.82
	Def.	298.98	124.58	71.49	140.18	85.13	58.40
	$2 \times \text{CO}_2$	301.26	167.16	100.38	160.89	106.55	58.47
	Joint	301.63	131.81	76.86	144.25	88.63	59.23
S.E. Asia	Ctl.	297.55	263.29	183.76	149.64	112.02	41.78
	Def.	297.35	243.21	164.78	137.71	100.61	40.84
	$2 \times \text{CO}_2$	299.93	264.86	181.33	155.04	114.55	44.78
	Joint	299.61	248.08	167.95	141.69	102.19	43.33
Africa	Ctl.	299.80	123.19	70.20	146.80	85.23	65.01
	Def.	299.79	117.96	64.98	137.13	79.07	61.32
	$2 \times \text{CO}_2$	302.57	127.35	72.84	151.89	86.03	66.39
	Joint	302.32	125.29	71.48	141.58	83.20	61.82

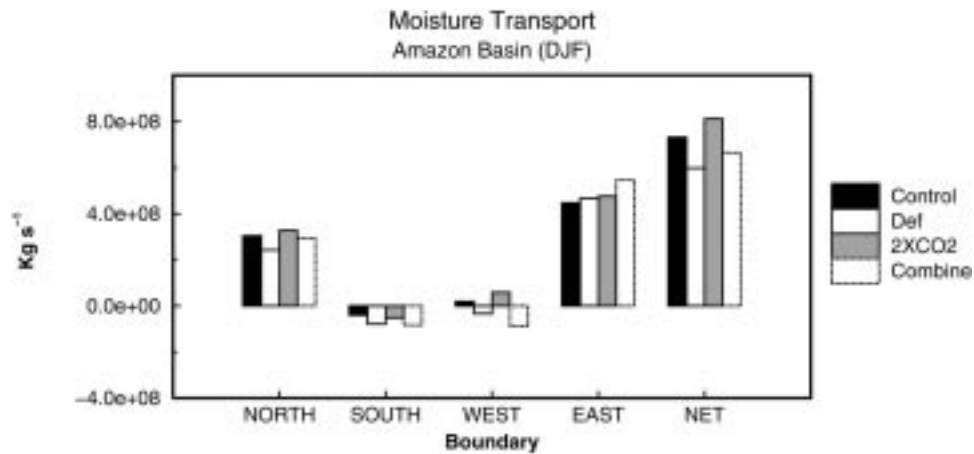


Figure 3. Vertically integrated incoming water vapour over the domain of Amazon Basin in the seasonal averages of December–January–February in the four sets of experiments.

surface and results in a large increase in surface temperature of about +3.0 K. For surface energy balance, the additional surface energy is balanced by the increase of surface sensible heat and the net outgoing longwave radiation away from the warmed land surface.

Joint surface climate changes over Southeast Asia are qualitatively similar to those over the Amazon Basin. Annually averaged evapotranspiration is decreased by $-9.8 \text{ mm month}^{-1}$, less than the reduction in total precipitation ($-15.2 \text{ mm month}^{-1}$). Thus, the incoming moisture transport is weakened over Southeast Asia land areas. As for the Amazon Basin, a warmer surface (+2.1 K) is simulated in Southeast Asia. It should be noted that as a simple slab ocean model is applied in this study, the impacts of such land-surface warming on the monsoon circulation may not be adequately represented due to a weak air-sea interaction in the model. This can in part explain the small change of monsoon precipitation in the joint experiment.

Surface climatic changes over tropical Africa are much weaker than those in the Amazon and Southeast Asia. Surface total evapotranspiration over tropical Africa is decreased ($-2.0 \text{ mm month}^{-1}$). In contrast to the changes in the Amazon Basin and S.E. Asia, rainfall over tropical Africa is increased by $+2.1 \text{ mm month}^{-1}$ in response to the joint effect of greenhouse warming and deforestation. As surface evapotranspiration is reduced (indicating a weakened local water recycling), the increase in precipitation can only be interpreted as an enhancement of incoming water vapour transport from nearby regions. Another difference in the results for tropical Africa is that the surface sensible heat flux is reduced by -3.2 W m^{-2} , while the ground surface temperature is increased by +2.5 K. Model analysis shows that the increase in surface air temperature is even larger than the increase in ground surface temperature, indicating that the temperature gradient between the land and the surface air is weakened, explaining the reduction in surface sensible heat flux.

3.2. CHANGES IN ENERGY BUDGETS AND REGIONAL WATER VAPOUR TRANSPORT

From the radiation point of view, deforestation causes change in absorbed short-wave radiation at the land-surface due to the imposed increase in surface albedo, while the major impacts of greenhouse warming are the changes of atmospheric longwave radiation both towards surface and out to space. In addition, deforestation alters the surface radiative energy partition between latent and sensible heat fluxes and thus affects the surface moisture and thermal properties. Therefore, analysing the surface and atmospheric energy budgets is potentially an instructive means of exploring the physical links between deforestation and greenhouse warming. As the previous section suggests similar changes over three tropical rainforest regions, only the analysis for the Amazon Basin is presented here.

Figure 2a illustrates the annually averaged changes of surface and atmospheric energy budgets between the 10-year joint experiment and 25-year control exper-

iment. The influence of deforestation on the radiative processes is seen in two aspects of the results. The shortwave radiation reflected from the surface to the atmosphere S_r is increased by $+16.9 \text{ W m}^{-2}$ due to the increase in surface albedo. More solar radiation is returned to space from the top of the atmosphere (TOA) in spite of the reduction of total cloud cover.

The effect of doubling the atmospheric CO_2 concentration is seen in the large changes in the longwave radiation components. Downward longwave radiation from the atmosphere to the land-surface (F_a) and the outgoing longwave radiation at the top of the atmosphere (TOA) to space (OLR) are increased because the atmosphere is warmer as more longwave radiation is absorbed by the increased atmospheric CO_2 concentration. The fact that the increase of F_a ($+13.8 \text{ W m}^{-2}$) is larger than that of OLR ($+10.0 \text{ W m}^{-2}$) suggests that greenhouse warming effect is mainly confined to the lower levels of the atmosphere, as seen in other GCM simulations (cf. Houghton et al., 1990, 1992, 1996).

In the joint experiment, changes of surface energy budget are complicated by the interactions between processes induced by tropical deforestation and processes induced by the doubled- CO_2 concentration in the atmosphere. In terms of the changes of longwave radiation, the land-surface loses energy as the increase of outgoing longwave radiation from the land-surface ($F_s = +19.9 \text{ W m}^{-2}$) is larger than the increase of downward longwave radiation from the atmosphere to the surface ($F_a = +13.8 \text{ W m}^{-2}$): the net upward longwave radiation from the surface is increased by $+6.1 \text{ W m}^{-2}$. Taking into account the increase of surface reflection of solar radiation and the loss of energy from surface longwave radiation, it is clear that the reduction of surface evaporation due to tropical deforestation makes a significant contribution to maintaining the warmed land-surface in the joint experiment.

This feature is different from the changes in surface and atmosphere energy budgets in the $2 \times \text{CO}_2$ experiment. Figure 2b, which illustrates the changes of energy budget terms between the $2 \times \text{CO}_2$ and control experiments, shows that doubling of atmospheric CO_2 concentration in the atmosphere leads to an increase of longwave radiation from the overlying atmosphere to the land-surface (F_a) by $+18.8 \text{ W m}^{-2}$ which is larger than the increase of outgoing longwave radiation from land-surface to the atmosphere ($+15.7 \text{ W m}^{-2}$). The net outgoing longwave radiation between the land-surface and the atmosphere is decreased by -3.1 W m^{-2} due to the doubling of atmospheric CO_2 concentration, and hence results in a warmer land-surface.

Following the above analysis, it must, however, be pointed out that the large increase in surface temperature in the joint experiment is not solely caused by the reduction of surface evapotranspiration. Even though the net longwave radiation released by the surface ($F_s - F_a$) in the joint experiment is increased by $+6.1 \text{ W m}^{-2}$, the enhanced downward longwave radiation (F_a) increases the surface absorbed radiative energy and contributes to the large surface warming. Otherwise, as seen in the deforestation-alone experiment (cf. Zhang et al., 1996a) deforestation results in

the reduction of cloud cover, reducing the longwave radiation from the atmosphere to the surface and allowing more outgoing longwave radiation to be lost from the surface to space. In that case, the net loss of longwave radiation nearly offsets the changes in surface net solar radiation and surface evaporation. Consequently, a small change in the surface temperature was simulated in the deforestation-alone experiment.

Thus, the large increase of surface temperature in the joint experiment is not an individual effect from either the increase in CO₂ concentration or deforestation but the combination of both: the reduction of land-surface latent heat flux induced by tropical deforestation and the increase in downward longwave radiation from the atmosphere to the land-surface as a result of the increased atmospheric CO₂ burden. This analysis clearly demonstrates the highly interactive nature of the climate system. In the joint experiment, the processes of greenhouse warming and deforestation affect each other. Reduction of cloud cover, largely due to the effect of deforestation, not only weakens the effect of the increase in surface albedo by allowing more solar radiation to reach the land-surface during the day-time, but also modifies the longwave radiation between the land-surface and the atmosphere by allowing more outgoing longwave radiation to be lost by the warmed land-surface. At the same time, reduction of surface latent heat flux can offset the loss of outgoing longwave radiation by the reduction in cloud cover and makes a large contribution to maintaining the increased surface temperature.

With the changes in the surface and atmospheric energy budgets as well as the atmospheric boundary layer conditions following deforestation, regional atmospheric circulation are affected also. Imposing tropical deforestation on the current model climate, Zhang et al. (1996) identified that tropical deforestation could lead to changes in regional atmospheric circulation and that moisture transport over the deforested regions was affected by the changes in land-surface properties. This finding is re-investigated by assessing the change in water vapour transport following tropical deforestation and doubling atmospheric CO₂ concentration. Figure 3 shows the vertically integrated water vapour transport over the domain from 20° S to 5° N and 75° W to 40° W, roughly covering the Amazon Basin:

$$F_q = -\frac{1}{g} \int_{P_s}^{P_o} \left[\oint (q * V_n) ds \right] dP, \quad (1)$$

where P_s and P_o are the surface and model top-level pressures, respectively. V_n is the horizontal wind component normal to the corresponding boundary and q is specific humidity, and ds is the path length at each of the four boundaries in the domain defined. During DJF, the wet season in the Amazon Basin, it is seen that following tropical deforestation and greenhouse-warming in the joint experiment, incoming water vapour on the northern boundary associated with the ITCZ is weakened. The western boundary, which is a moisture source for the Basin in the control experiment, becomes a moisture sink as atmospheric water vapour is blown out of the basin by the increased low-level wind following the reduction of surface roughness

due to deforestation. On the southern boundary, more atmospheric water vapour is transported out of the basin. Despite the fact that the incoming water vapour across the eastern boundary of the Basin is increased in the joint experiment, the net effect is such that overall incoming water vapour transport is reduced as compared with the control experiment. The reduction in the net incoming water vapour transport explains the reduction in total precipitation which is larger than the reduction in surface evaporation in the joint experiment.

Analysis of changes in water vapour transport over the Amazon Basin following deforestation and greenhouse-warming suggests that the response of local and regional atmospheric circulation can worsen the consequences of tropical deforestation. The regeneration of secondary forests following deforestation in a greenhouse-warmed climate is likely to be detrimentally affected by a drier climate not only due to the weakening of water recycling (forest evapotranspiration) but also by the reduction of atmospheric water vapour transport into the region and hence lowered precipitation.

4. Impacts of Tropical Deforestation in a Greenhouse-Warmed Climate

This section is designed to assess the impacts of tropical deforestation in the greenhouse-warmed climate over tropical rainforest regions. First, differences between the joint experiment and the $2 \times \text{CO}_2$ experiment are analyzed to show how the local climate under greenhouse warming is affected by tropical deforestation over the Amazon Basin, Southeast Asia and tropical Africa. Then, regional climate changes are compared with those in the deforestation experiment of Zhang et al. (1996a,b) (the impacts of tropical deforestation on the present-day climate) to determine whether the impacts of tropical deforestation may be affected by greenhouse warming.

4.1. THE AMAZON BASIN

To estimate the influence of tropical deforestation on a greenhouse-warmed climate, it is necessary first to analyze how regional climates over the tropical rainforest regions are affected by doubling the atmospheric CO_2 concentration. As shown in Table I, regional climate changes over the Amazon Basin in the $2 \times \text{CO}_2$ experiment comprise an increase in surface temperature of +2.6 K and an increase in regional precipitation of about +9.0 mm month⁻¹, of which 3.3 mm month⁻¹ is contributed by an increase in convective precipitation. Increasing the atmospheric CO_2 concentration leads to an increase in the net longwave radiation at the land-surface (of about 4.5 W m⁻²) and, consequently, increases in surface evapotranspiration and sensible heat flux.

Seasonal variations of surface climate changes over the Amazon Basin between the four sets of experiments conducted in this study are shown in Figure 4. There

TABLE II

Changes in the surface climate over three tropical deforested regions in both pairs of deforestation experiments: Deforestation with present-day climate conditions (present); Deforestation with greenhouse warmed climate conditions (greenhouse). P is the monthly total precipitation (mm month⁻¹); E the monthly total evapotranspiration (mm month⁻¹); T_s the surface air temperature (K); R the surface net radiation (W m⁻²); H_s the surface sensible heat flux (W m⁻²). Results are the areal averages over the regions shown in Figure 1

		P	E	T_s	R	H_s
Amazon	Greenhouse	-35.35 (-21.2%)	-17.91 (-16.8%)	+0.38	-16.64	+0.77
	Present	-33.61 (-21.2%)	-18.45 (-17.8%)	+0.29	-16.24	+1.58
S.E. Asia	Greenhouse	-16.77 (-6.3%)	-12.36 (-10.8%)	-0.32	-13.35	-1.45
	Present	-20.08 (-7.6%)	-11.41 (-10.2%)	-0.20	-11.93	-0.94
Africa	Greenhouse	-2.05 (-1.6%)	-6.00 (-6.9%)	-0.25	-10.32	-4.57
	Present	-5.23 (-4.2%)	-6.16 (-7.2%)	-0.01	-9.67	-3.69

are four combinations between them: difference between joint and control experiments represents the joint impacts of deforestation and greenhouse arming; difference between joint and $2 \times \text{CO}_2$ experiments represents the impacts of deforestation in the greenhouse-warmed climate; difference between $2 \times \text{CO}_2$ and control experiments shows the climatic changes due to greenhouse warming; and the difference between deforestation and control experiments demonstrates the impacts of deforestation in the current climate condition. The difference between the results of the $2 \times \text{CO}_2$ and control experiments illustrates that the increases in surface temperature and monthly total precipitation occur throughout most of the year with the largest increment in precipitation (about +20.0 mm month⁻¹) in the local wet season of February, March, October and November. Greenhouse warming leads to an increase in surface evapotranspiration of about 3–5 mm month⁻¹ in most months. Overall, doubling the atmospheric CO_2 concentration leads to a warmer and wetter climate over the Amazon Basin.

Annually averaged impacts of tropical deforestation on the present-day and greenhouse-warmed climates are shown in Table II. Impacts of deforestation on the present-day climate are the same as presented in Zhang et al. (1996a). Over the Amazon Basin, the response of the greenhouse-warmed climate to tropical deforestation shows very similar features to those seen for a present-day deforestation experiment. Removal of the tropical rainforest in the greenhouse-warmed climate leads to a reduction in surface evapotranspiration by $-17.9 \text{ mm month}^{-1}$ and a reduction in total precipitation by $-35.4 \text{ mm month}^{-1}$. The increase in surface albedo following deforestation results in the reduction of surface net radiation by -16.6 W m^{-2} and surface temperature shows only a small increase ($+0.4 \text{ K}$) as

reductions in surface solar radiation and surface evapotranspiration tend to cancel each other.

Overall, annually averaged climate changes induced by tropical deforestation do not differ greatly in the present-day and in the greenhouse-warmed world. The main reasons are likely to be that: (1), as summarised in the IPCC scientific reports (Houghton et al., 1990, 1992, 1996), the largest impacts of doubling the atmospheric CO₂ concentration are located in the middle and high latitudes, especially for changes in surface temperature; and (2) CCM1-Oz's response to doubling the CO₂ concentration in the atmosphere lies towards the lower end of the IPCC range of sensitivities (cf. Henderson-Sellers et al., 1995; Howe and Henderson-Sellers, 1997).

The seasonal distribution of surface climate changes in the two sets of deforestation experiments has similar features as shown in Figure 4. In the greenhouse-warmed climate, deforestation produces an overall increase in surface temperature throughout the year of about +0.3 to 0.5 K. Reductions in total precipitation are simulated in most of the months. The largest reductions occur during the periods of February–March–April–May (–45.9 mm month⁻¹) and September–October–November–December (–49.1 mm month⁻¹). The effect of the increase in surface albedo leads to a reduction of surface net radiation of –15 to –20 W m⁻² with no obvious seasonal variations. A decrease in surface evapotranspiration of about –15 to 20 mm month⁻¹ is seen throughout the year, while surface sensible heat flux does not show large and coherent changes.

Results from Figure 4, which are the averages over the whole deforestation area in the basin, may have missed some detailed regional features. Thus, results from the model simulations in January between 10-year joint and 2 × CO₂ experiments are shown in Figure 5. Deforestation imposed into the greenhouse-warmed climate results in a large reduction in surface evapotranspiration over much of the basin. Changes over the western part of the basin are about –20.0 W m⁻² (Figure 5a). Surface temperature (Figure 5c) is slightly increased over the Amazon Basin and also shows a large increase (about +1.0 K) over eastern Brazil and a decrease over the southern continent (25° to 35° S). Those changes are statistically significant at 95% confidence level using the classic Student's *t* test. When changes are statistically significant at this level, it means the model-simulated changes are more than twice as large as model's internal variation. Rainfall over the western Amazon Basin and over eastern Brazil is decreased by over –50 mm month⁻¹ (Figure 5b), but no significant changes are found over the Amazon Basin. The heterogeneity of the changes in surface temperature and precipitation is the reason why the areal averaged changes over the whole basin is weaker in January as seen in Figure 4. In addition, the increase in precipitation in the 25° to 35° S latitude region, together with the changes in surface temperature over the same area, indicate that deforestation over the Amazon Basin under the greenhouse-warmed climate can result in regional impacts beyond the deforested region as previously seen in Zhang et al. (1996a) for the present-day climate.

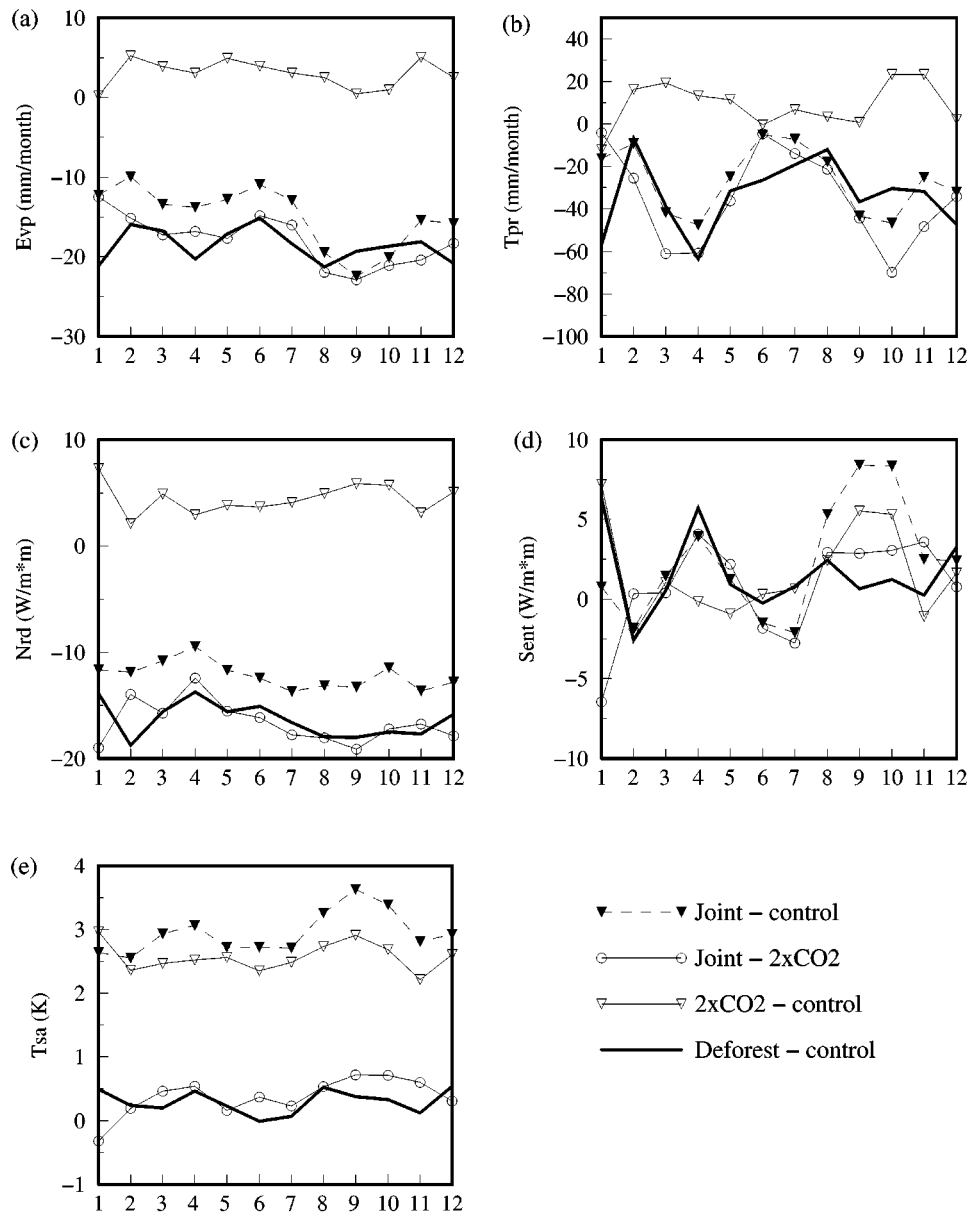


Figure 4. Regionally averaged climate changes over the Amazon Basin between the four experiments used in this study: *Evp* (evapotranspiration); *Tpr* (precipitation); *Nrd* (net surface radiation); *Sent* (sensible heat flux); and *Tsa* (surface temperature).

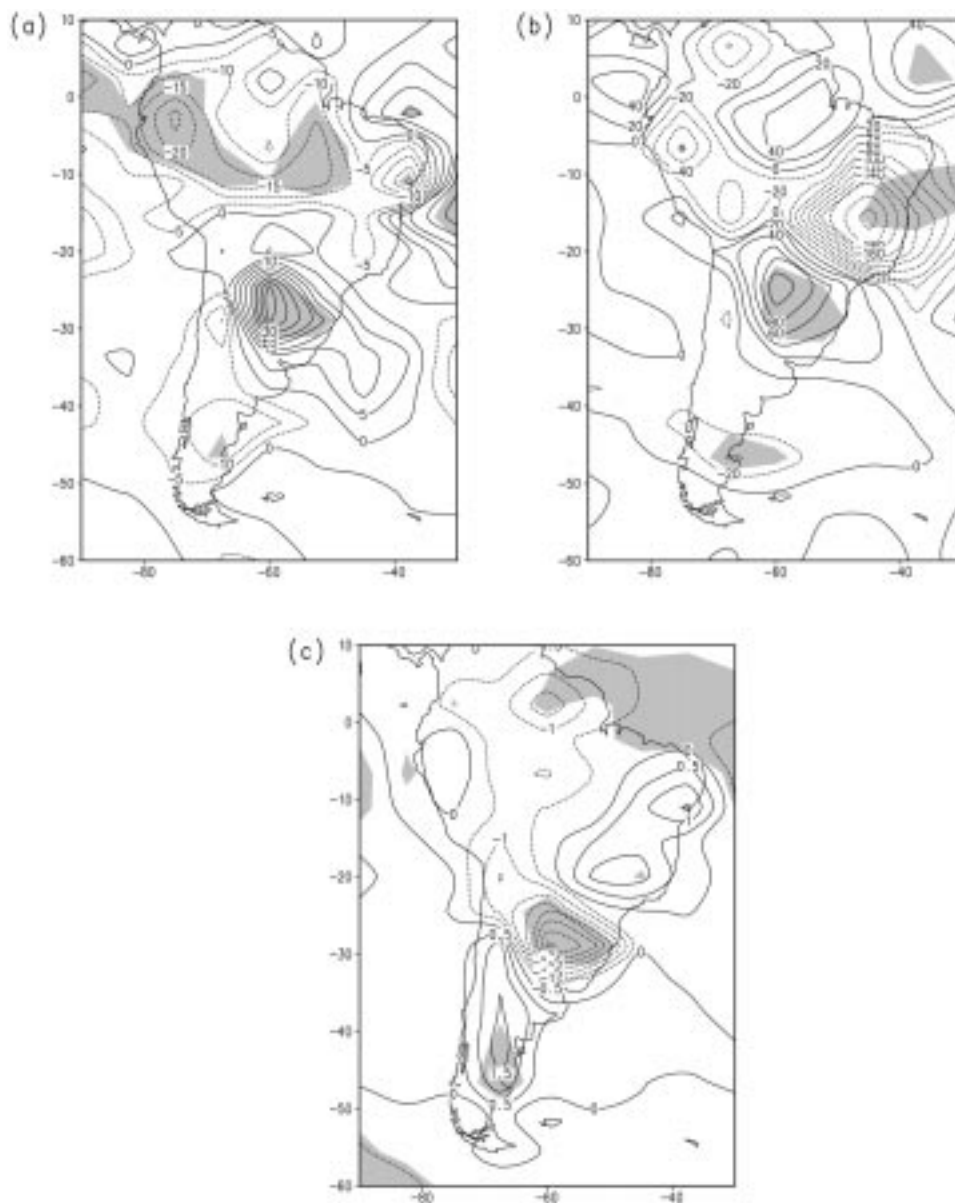


Figure 5. Geographical distribution of surface climate changes over South America in January between the 10-year joint and $2 \times \text{CO}_2$ experiments. Shaded areas indicate changes are statistically significant at the 95% confidence level by using the Student's *t* test. (a) Changes in surface evapotranspiration with a contour interval of 5 mm month^{-1} . (b) Changes in total precipitation with a contour interval of 20 mm month^{-1} ; (c) Changes in surface temperature with contour interval of 0.5 K.

4.2. SOUTHEAST ASIA AND TROPICAL AFRICA

Meehl and Washington (1993) noted, using a coupled ocean-atmosphere global climate model, that greenhouse warming may enhance the Asian summer monsoon, in part due to the intensified land and ocean temperature contrast. In CCM1-Oz, which has only a simple mixed-layer ocean, the land-surface climate over Southeast Asian continents appears to be fairly insensitive to the greenhouse forcing, except for the increase in surface temperature of +2.4 K (Table I). Total precipitation is slightly increased (by +1.6 mm month⁻¹) and evapotranspiration is increased by +2.5 mm month⁻¹. The seasonal variations of changes in the areal averaged surface variables in the four experiments are shown in Figure 6. Surface temperatures increase throughout the year by about +2.0 to +2.5 K by doubling CO₂ concentration. Precipitation does not show systematic changes during the course of the year: the largest increase (+61.0 mm month⁻¹) occurs in May and the largest reduction (−74.0 mm month⁻¹) in August. In addition, surface net radiation and evapotranspiration both are increased in almost every month with annually averaged increases of +5.4 W m⁻² and +2.5 mm month⁻¹, respectively.

Impacts of deforestation on the greenhouse-warmed land areas of Southeast Asia include a reduction in annually averaged surface evapotranspiration by −11.9 mm month⁻¹ (Table I) with smaller reductions in the local dry season from November to March (Figure 6). Total precipitation decreases in most months by −10 to −50 mm month⁻¹. Annually averaged total precipitation is reduced by −16.8 mm month⁻¹ and a large reduction in precipitation in the earlier summer monsoon (May–June–July) season is seen in the decrease of −40 mm month⁻¹. Land-surface temperature is decreased in most months with an annual averaged change of −0.3 K. The effect of the increase in surface albedo is seen in the large reduction of surface net radiation throughout the year (about −13.4 W m⁻²). As for Amazonia, the climatic impacts of tropical deforestation on the greenhouse-warmed climate and on the present-day climate have similar features over Southeast Asia (Table II): the reduction in annually averaged precipitation is slightly weakened in the greenhouse climate but changes in the other surface climate fields are similar. As shown in Figure 6, changes of surface evapotranspiration, sensible heat flux and surface air temperature have very similar seasonal patterns in the two pairs of Southeast Asian deforestation experiments.

Over tropical Africa, greenhouse warming leads large increases in surface temperature throughout the year (Figure 7) with an annual average of +2.8 K (Table I). Local rainfall under greenhouse-warmed condition displays increases in most months while reductions in precipitation are seen in August, September, November and December. Overall, annual averaged precipitation over tropical Africa is increased by +4.2 mm month⁻¹. Doubling the CO₂ concentration in the atmosphere leads to an increase of surface net radiation of about +5.0 W m⁻² throughout the year which, in turn, leads to an increase in surface evapotranspiration, together with an increase in local precipitation.

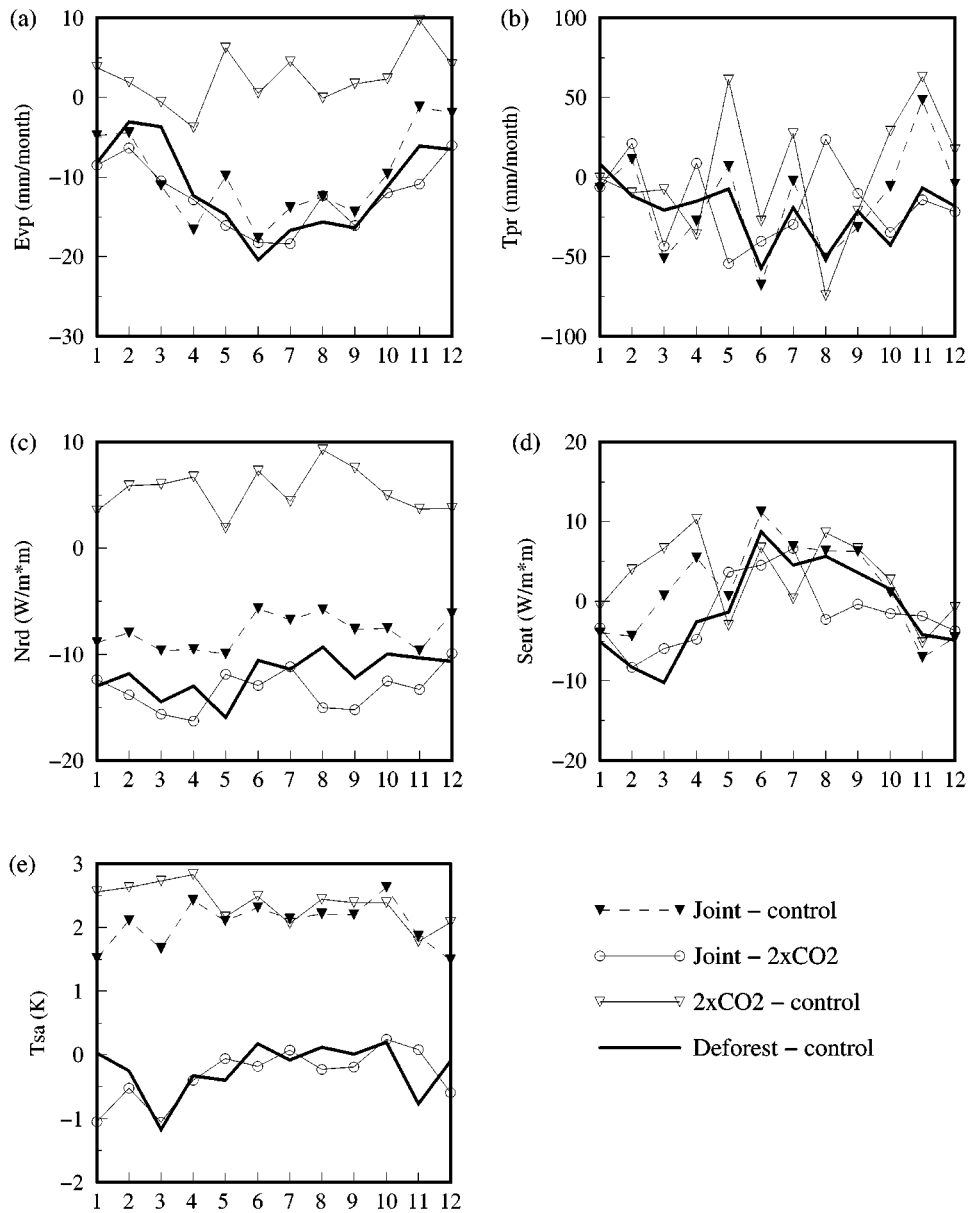


Figure 6. As Figure 4 but over Southeast Asia.

Deforestation in the greenhouse-warmed climate causes a reduction of surface evapotranspiration by about $-6.0 \text{ mm month}^{-1}$ in average and a reduction of surface net radiation by -10.0 W m^{-2} over tropical Africa. Total precipitation is reduced in most months (by -10 to $-20 \text{ mm month}^{-1}$): the exceptions being January, April, June and September. Surface air temperature appears to be decreased

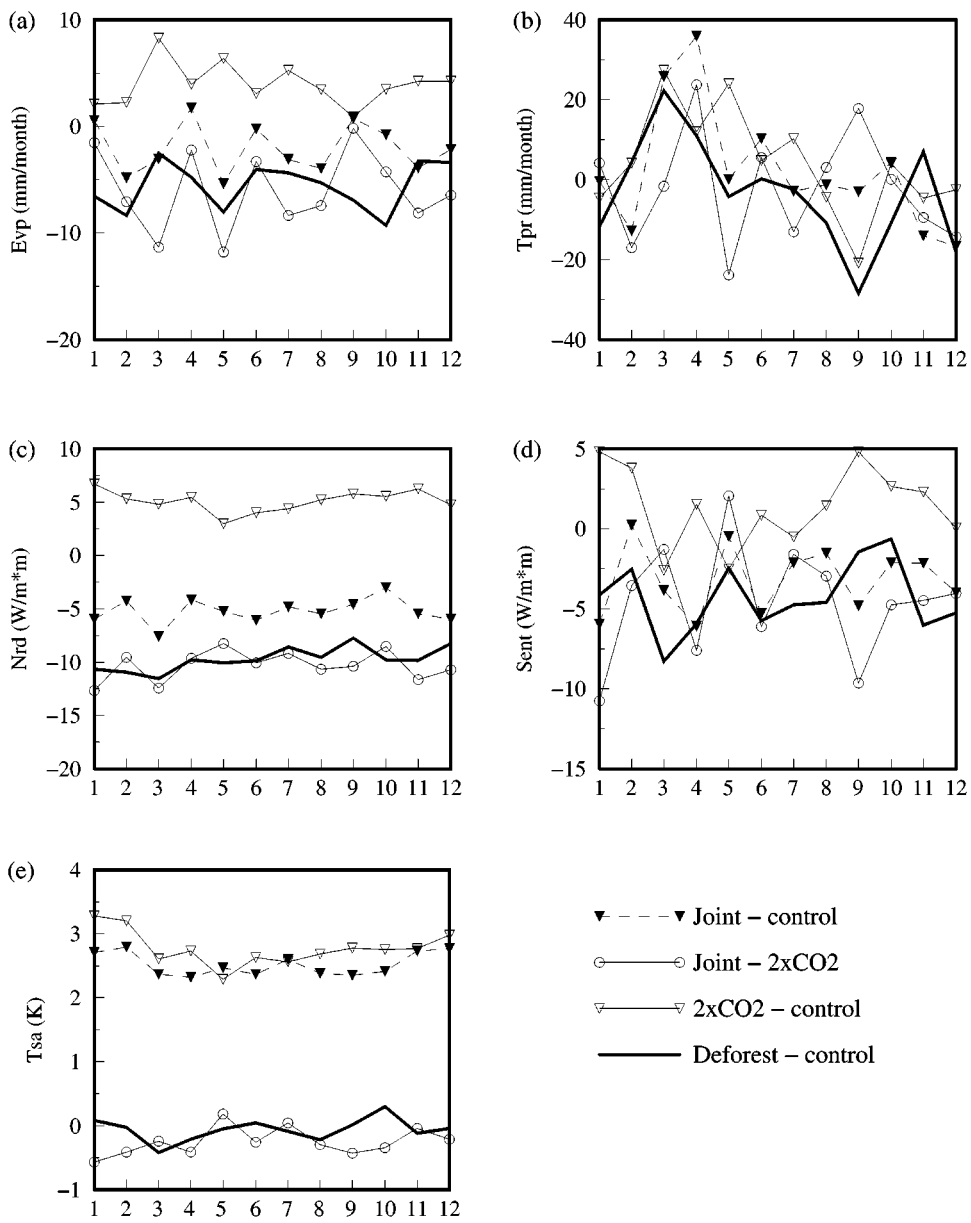


Figure 7. As Figure 4 but over tropical Africa.

by about -0.3 K in most months except May–June–July. Figure 7 shows that seasonal variations of changes in surface evapotranspiration due to deforestation are enlarged in the greenhouse-warmed climate. Changes in surface net radiation are quite similar in two sets of deforestation experiments. Surface temperature changes are different in the periods of January–February and September–October. During these periods surface air temperature is decreased following deforestation in the greenhouse-warmed climate but it is increased when deforestation is imposed in present-day climate. In February–March and August–September–October changes of precipitation show opposite signs between the pair of experiments.

Overall, local climate changes induced by tropical deforestation in greenhouse-warmed climate are similar to those induced in the present-day climate condition. Seasonal variations of changes over individual regions may be influenced. In some months, changes in surface temperature and precipitation have opposite signs in the two pairs of deforestation experiments.

5. Global Impacts of Tropical Deforestation in a Greenhouse-Warmed Climate

Zhang et al. (1996b), Sud et al. (1996) and Zeng et al. (1996) all discussed the possibility that tropical deforestation might induce large-scale climate disturbances. This section serves a dual purpose. Firstly we revisit the hypothesis that large-scale tropical deforestation may induce climate response distant from the deforested regions (e.g., in middle and high latitudes). This analysis also provides a chance to assess how the greenhouse climate signal could be distorted by the impacts of land-use change. The other purpose is to ascertain whether the greenhouse-warmed climate intensifies or reduces the potential impacts of tropical deforestation on the climate of extra-tropics. As reported in the IPCC Second Assessment (Houghton et al., 1996), the largest greenhouse-induced warming in most GCM simulations occurs over continental regions in the middle and high latitudes. Thus the atmospheric general circulation (especially the meridional Hadley circulation) is expected to be affected by the changes in the meridional temperature gradient and this could, in turn, modify the impacts of tropical deforestation in the middle and high latitudes.

Figure 8 shows changes of 500 hPa velocity potential between the 10-year joint experiment and 10-year $2 \times \text{CO}_2$ experiment in January and July. Changes of velocity potential in Figure 8 reflect planetary-scale responses of atmospheric circulation in the middle of troposphere to the tropical deforestation forcing imposed. Note that such large-scale changes cannot be directly linked to changes of surface climate (e.g., precipitation and temperature) over specific regions which are determined by complex interactions between atmospheric dynamics and physics represented in the model. However, results do suggest that imposing a large-scale tropical deforestation forcing in the model $2 \times \text{CO}_2$ climate can induce statistically significant (with 95% confidence level) responses in the large-scale atmospheric

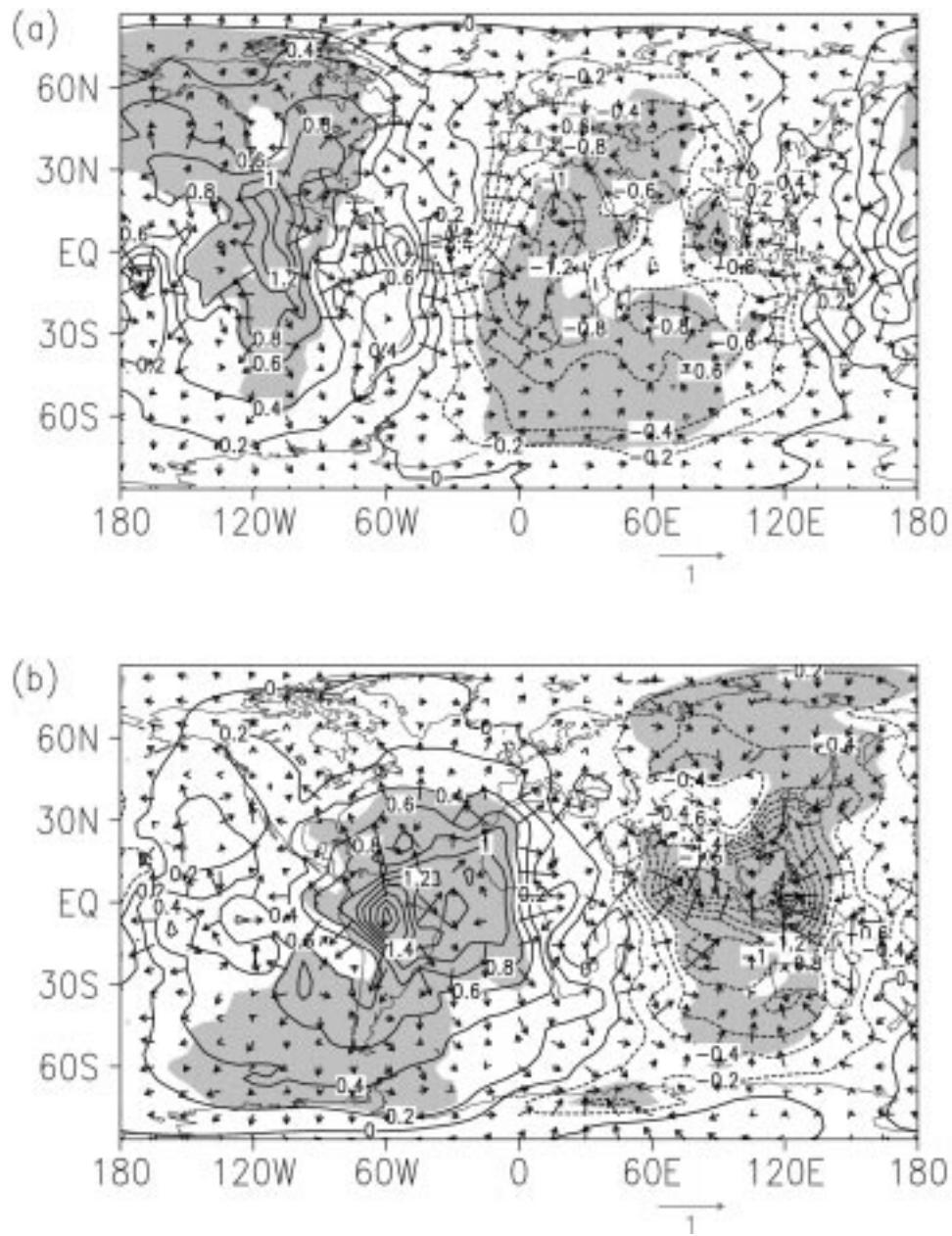


Figure 8. Changes of 500 hPa velocity potential ($\text{m}^2 \text{ s}^{-2}$) and its associated divergent flow (arrow) between the joint experiment and $2 \times \text{CO}_2$ experiment (contour interval: $5 \times 10^5 \text{ m}^2 \text{ s}^{-2}$). Shaded areas indicate the change of velocity potential is statistically significant at 95% confidence level: (a) January; (b) July.

circulation, not only in the tropics but also in the middle and high latitudes. Regions with significant changes of horizontal divergent and convergent flows in the tropics in both January and July indicate the likely response of tropical Walker circulation to the tropical land-surface disturbance. For instance, tropical deforestation induces divergent flow over the South American continent and over the eastern Pacific Ocean in the mid-troposphere, accompanying with convergent flows over tropical Atlantic Ocean and S.E. Asia. Climatologically, the upward branches of tropical Walker circulation are located over the tropical rainforest regions. It is therefore reasonable to expect that the changes of land-surface condition over large tropical forest regions might affect the overlying dynamical features. In addition, the changes in the middle and high latitudes seen in Figure 8 are of systematic feature and statistically significant at 95% confidence level using the simple classic *t* test. These changes suggest that the large-scale atmospheric circulation changes are not constrained in the tropics. They serve as a reason for attributing the statistically significant changes of surface climate in the extra-tropics, seen in the two sets of deforestation experiments reported here and discussed in Zhang et al. (1996b), to the model climate response to tropical deforestation rather than the model internal variability.

Middle and high latitude changes seen in Figure 8 are supported by the changes of vertically integrated kinetic energy and potential energy as shown in Figures 9 and 10. Both figures demonstrate that deforestation may alter the dynamic aspects of the GCM used in the study. There are statistically significant changes of kinetic energy over deforested regions in the Amazon Basin in July and over Southeast Asia and subtropical Africa in January. Systematic changes are also identified in the middle and high latitudes. In January, the Southern Hemisphere has more regions with statistically significant changes of vertically integrated kinetic energy than those in the Northern Hemisphere. This feature is reversed in July. Such results are physically reasonable as the upward branches of the meridional Hadley circulation are located in the Southern Hemisphere in January. The Hadley circulation can transfer the low-level atmospheric responses to the surface disturbance aloft into the middle and high-level atmosphere and then trigger middle and high latitude responses through wave propagation.

The changes of potential energy (Figure 10) reinforce the results seen in Figure 9. In Figure 10, it is seen that besides the significant changes in the tropics, there are large changes of potential energy in extra-tropics in both hemispheres. Furthermore, the changes in the middle and high latitudes resemble wave propagation features as first suggested by Zhang et al. (1996b). For instance, in January, there is a clear wave propagation pattern from the Amazonian region towards higher latitudes in both hemispheres. The changes of potential energy have negative-positive-negative-positive pattern from the tropics to the northeast Pacific Ocean, the North American continent and north polar region. In the Southern Hemisphere such a negative-positive-negative pattern is also observed from the tropics to the southeast Pacific Ocean and south of the South American continent. Comparing

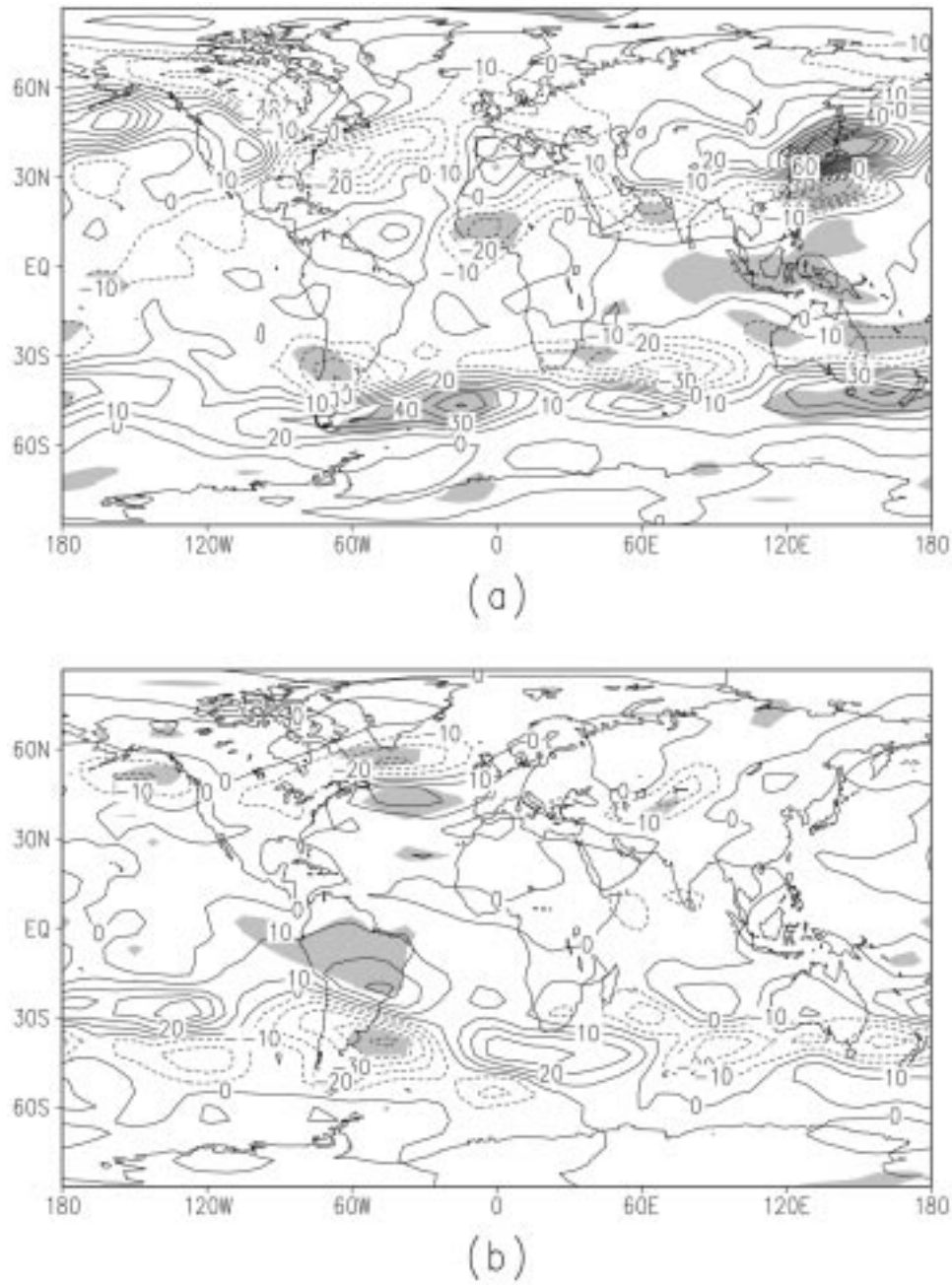


Figure 9. As Figure 8 but for vertically integrated kinetic energy (J m^{-2}).

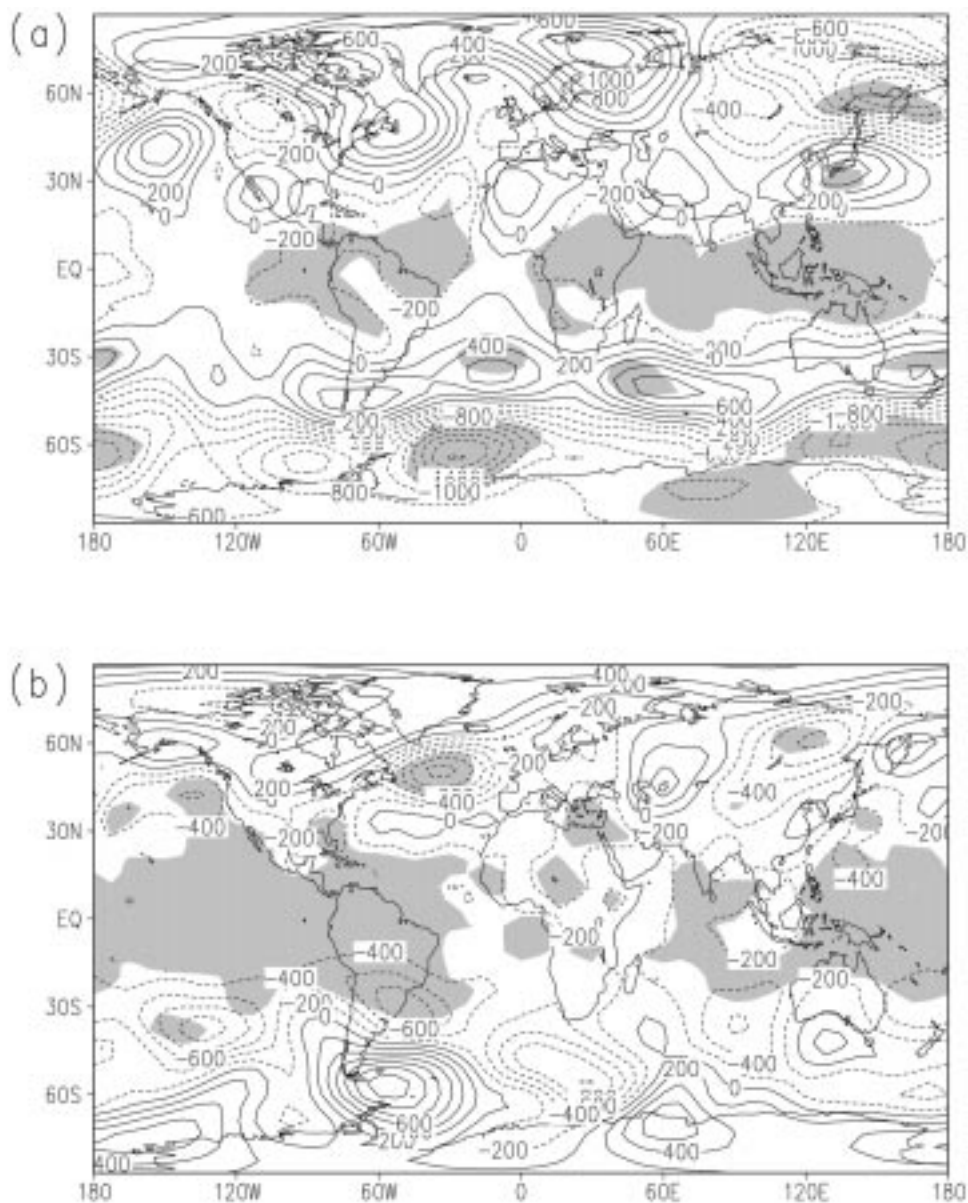


Figure 10. As Figure 8 but for vertically integrated potential energy (J m^{-2}).

Figures 10a,b indicates that the wave patterns are more pronounced in the winter hemisphere than in the summer hemisphere, which is in consistent with the theory of Rossby wave propagation (e.g., Webster, 1982).

From these results, it is seen that tropical deforestation forcing imposed in the greenhouse-warmed climate is capable of producing climatic disturbances dis-

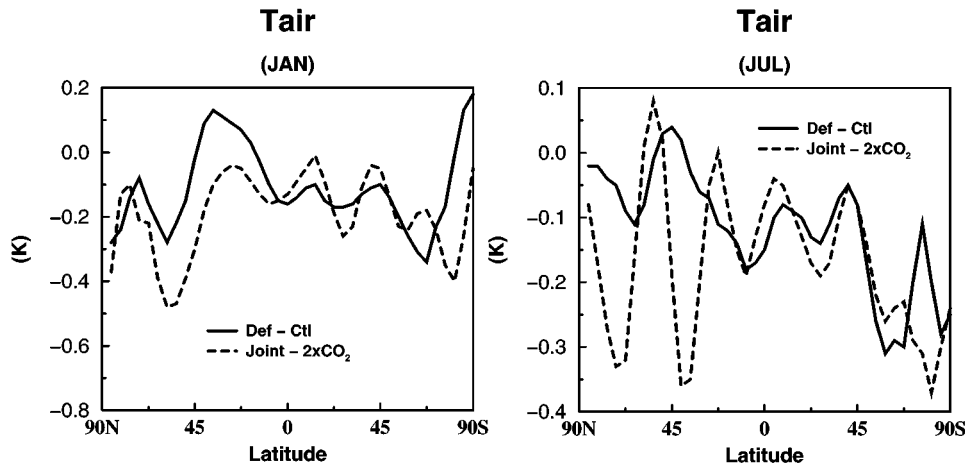


Figure 11. Zonal averaged surface air temperature changes in two pairs of deforestation experiments: (a) January; (b) July. Solid line (Def - Ctl) represents the changes between deforestation and control experiments, and dashed line (Joint - $2 \times \text{CO}_2$) represents the differences between the joint and $2 \times \text{CO}_2$ experiments.

tant from the deforested regions. This reinforces the results of previous studies (e.g., Zhang et al., 1996b; Sud et al., 1996). As stated in IPCC Second Assessment (Houghton et al., 1996), increasing atmospheric CO_2 concentration leads to changes in global atmospheric circulation and global water and energy cycles. Here, we compare whether the extra-tropical impacts of tropical deforestation are enhanced or weakened in the current climate condition and in the greenhouse-warmed climate condition in the model. Figure 11 shows the zonally averaged surface air temperature changes in the two pairs of deforestation experiments. Model results indicate that temperature changes in the Northern Hemisphere middle latitudes, which are caused by tropical deforestation, are enhanced in the greenhouse-warmed world. The cooling in the winter of the Northern Hemisphere middle latitudes (January) is increased from -0.2 to about -0.4 . In the Northern Hemisphere summer season (July), the cooling is increased from -0.1 to about -0.3 . The cooling effect induced by tropical deforestation in the middle latitudes of both hemispheres may be the result of the weakening of meridional Hadley circulation following deforestation as shown in Zhang et al. (1996b). This results in the meridional transport of tropical warm air being reduced. Temperature changes in the Southern Hemisphere are of similar magnitude and direction. It should be noted that other surface variables (e.g., surface evaporation, precipitation etc.) do not show any coherent signals suggesting whether extra-tropic impacts of deforestation are strengthened or weakened in the simulated greenhouse-warmed climate. The overall results from this study indicate that extra-tropical impacts of tropical deforestation in greenhouse conditions retain similar magnitudes to those simulated for the present day but suggest that regional signals may be different.

Finally, we try to assess to what extent tropical deforestation may affect the model-simulated global climate change resulting from the doubling of atmospheric CO_2 . Figure 12 displays changes of surface temperature following tropical deforestation in the $2 \times \text{CO}_2$ climate. Despite the fact that only a small part of the temperature differences are significant in a statistical sense, the overall extratropical temperature changes over land are above 1 K. Over Northern high latitudes the temperature signals are as large as 2 K. Such changes therefore possibly disturb the 'detection' of a greenhouse warming signal in the modelled climate. This suggests that to reduce the uncertainties in the GCM-simulated future climate change, impacts of land-use change to date and postulated for the future need to be taken into consideration.

6. Conclusion and Discussion

In this study, we have reported results from a series of GCM model simulations undertaken to try to assess the joint impacts of tropical deforestation and greenhouse warming on climate. By employing a version of NCAR Climate Community Model (CCM1-Oz), regional and global climatic changes in a 'worst case' scenario are presented in which doubling the atmospheric CO_2 concentration and tropical deforestation happen simultaneously. A warmer and drier climate is simulated over the Amazon Basin and Southeast Asia, while precipitation over tropical Africa is increased in the model. Analyses of changes in surface and atmospheric energy budgets demonstrate that the large increase in surface temperature in the joint experiment is the joint result of tropical deforestation and greenhouse warming. Both the increase in downward longwave radiation from atmosphere to surface (due to doubling CO_2 concentration) and the reduction in surface evapotranspiration (due to deforestation) make contributions to maintaining a warmed land surface over deforested regions. These two processes are closely coupled in the model physics.

To further examine the non-linearity in the model results, we compare the model-simulated combined climatic changes due to tropical deforestation and greenhouse-warming with the sum of the changes in the two experiments in which these two processes are applied separately. Figure 13 shows the difference between climatic changes in the joint experiment and the sum of climatic changes in the $2 \times \text{CO}_2$ experiment and deforestation experiment alone. Hereafter we name such a difference the 'non-linearity difference'. If the model has a predominantly linear response to the two imposed disturbances, then we expect the model non-linearity difference to be small. Figure 13 clearly demonstrates that the model's degree of linearity to these two processes (deforestation and doubling CO_2 concentration) is seasonally and regionally variable. In the Amazon Basin, the model linearity is stronger (differences close to zero) in the model's drier period (May to September). This is particularly true for the changes in surface net radiation and temperature. On the other hand, results of the differences in surface evaporation and total pre-

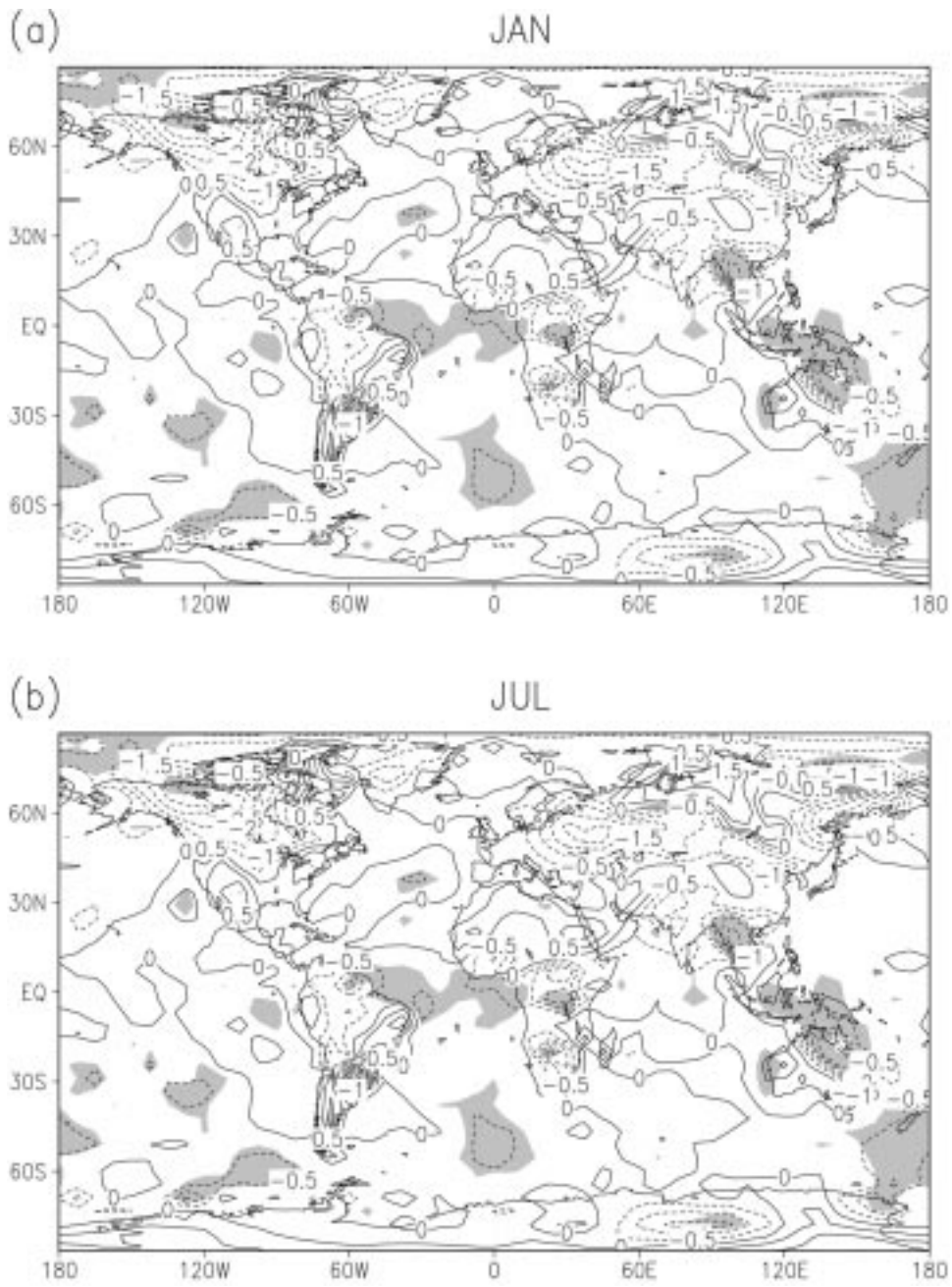


Figure 12. As Figure 8 but for surface air temperature (K).

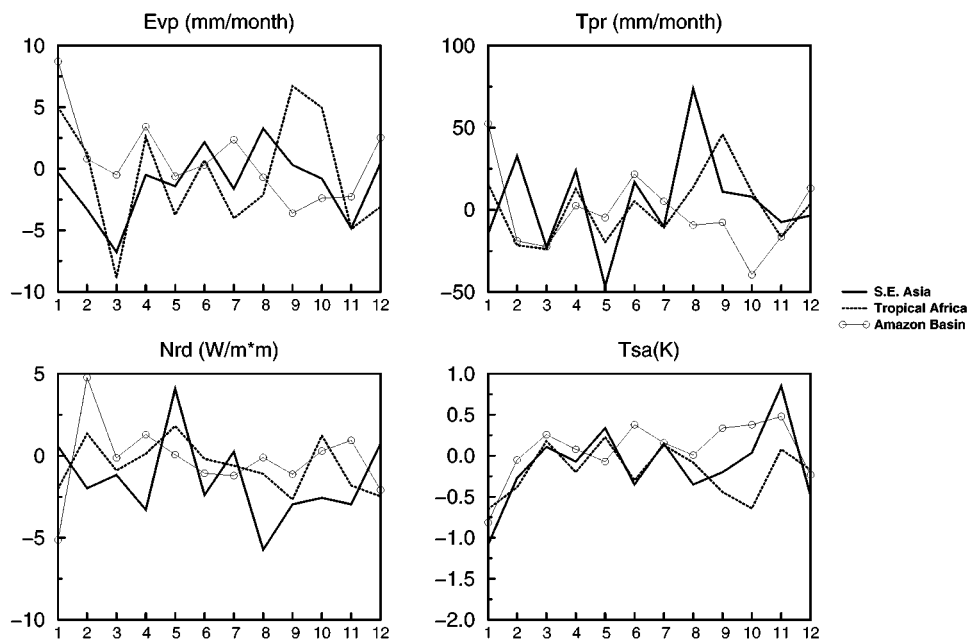


Figure 13. Differences between climate changes as a measure of linearity of model response. The change between the joint and control experiments is differenced from the sum of the changes in the separate deforestation and $2 \times \text{CO}_2$ experiments. *Evp* is the difference in monthly total evaporation; *Tpr* is the difference in monthly total precipitation; *Nrd* is the difference in monthly-averaged surface net radiation and *Tsa* is the difference in surface air temperature. Near zero values indicate linearity in model response while large values suggest non-linearities.

precipitation (and occasionally surface temperature) indicate that the non-linearity in the model results can be large in certain months. For instance, the non-linearity difference in monthly precipitation is as large as 50 mm month^{-1} in January and $-47 \text{ mm month}^{-1}$ in October, which are larger than the changes simulated in the joint experiment (cf. Figure 4). In S.E. Asia and tropical Africa, there are quite large non-linearity differences in the changes of surface evaporation in March, August and September when such differences are comparable in the changes seen in the three sets of experiments (cf., Figures 6 and 7). It is also noted that in a number of months the non-linearity differences in monthly total precipitation are larger than 25 mm month^{-1} which is comparable with the changes induced by deforestation and doubling CO_2 concentration. The non-linearity difference in the changes of surface temperature can be as large as 1.0 K in S.E. Asia which are also significant in terms of changes seen in the model deforestation and/or greenhouse warming experiment(s). Overall, the results in Figure 13 suggest that the model tends to perform more non-linearly than linearly in its response to the two imposed disturbances. This is consistent with the conclusion derived from the analysis of the changes in the surface and atmosphere energy budgets.

Furthermore, our results show that in the model-simulated greenhouse-warmed climate, annually averaged climatic changes due to deforestation over tropical rainforest regions retain similar characteristics as to those in which deforestation is imposed in the present-day climate (cf. Zhang et al., 1996a). Such a similarity between the pair of deforestation experiments could be due to the fact that the global warming signal in this model as in others (e.g., Howe and Henderson-Sellers, 1997) is weak in the tropics.

In this study we have found that tropical deforestation can lead to responses in large-scale atmospheric circulation. This reinforces the results from earlier GCM studies (e.g., Zhang et al., 1996; Sud et al., 1996). Zonally averaged results suggest that there are no systematic signals suggesting that large-scale impacts of deforestation on extra-tropics in general are enhanced in the greenhouse-warmed climate, though surface temperature changes in Northern Hemisphere are larger when deforestation is imposed in the $2 \times \text{CO}_2$ climate. It should be pointed out, however, that even though this finding is limited by the model used in the study, which has coarse resolution and a slab ocean, this study suggests that the scientific issues such as how land-use change may affect projections of future climate need to be addressed.

Henderson-Sellers et al. (1995) and other researchers have found that doubling the CO_2 concentration in models that capture additional land-surface attributes can produce smaller global climatic changes than a 'simple' greenhouse warming alone. Our results underline the suggestions of Pielke et al. (1998) that land-use change has, and is, compounding the greenhouse warming signal and hence rendering detection of the impacts of both effects very difficult. The hint of non-linearity in the responses found (e.g., Figure 13) further complicates this situation. Any conclusion as to whether the impacts of tropical deforestation may be enhanced by greenhouse warming is limited by this particular model simulation of the $2 \times \text{CO}_2$ climate and constrained by its uncertainties. Employing interactive canopy schemes in GCMs (e.g., Sellers et al., 1997; Cox et al., 1999) would enable us to further investigate land-use and future climate.

We conclude on a two-edged cautionary note. In this study we examined a worst case scenario for the tropical rainforest climate in which all the rainforest in the tropics is replaced by grassland in the model. Different deforestation scenarios might be used in the future to project the climate changes in these regions especially if these were believed to be more realistic. For instance, Fearnside (1996) pointed out that if current behaviour patterns remain unchanged in the Amazon Basin, then land-cover in the rainforest region could reach an equilibrium dominated by productive pasture and secondary forest derived from pasture. Similarly, continuous observational studies (e.g., Culf et al., 1995) also provide more realistic changes of surface parameters (e.g., albedo, roughness length and soil properties) to be used in future model studies which may also affect the model results (e.g., Pitman et al., 1993). However, the aspiration of 'realism' in tropical forest simulations may be difficult to achieve. The results we have presented here suggest that global

warming and forest removal or degradation compound, perhaps in non-linear ways. Together, the results of even modest warming and tree removal may already be modifying the 'reality' which careful observations are attempting to resolve, for example by altering the water vapour budget of the tropical forest regions (e.g., Figure 3). The real world is not a stationary goal.

References

- Cox, P. M., Betts, R. A., Bunton, C. B., Essery, R. L. H., Rowntree, P. R., and Smith, J.: 1999, 'The Impact of New Land Surface Physics on the GCM Simulation of Climate and Climate Sensitivity', *Clim. Dyn.* **15**, 183–203.
- Culf, A. D., Fisch, G., and Hodnett, M. G.: 1995, 'The Albedo of Amazonian Forest and Ranch Land', *J. Climate* **8**, 1544–1554.
- Dickinson, R. E., Henderson-Sellers, A., Kennedy, P. J., and Giorgi, F.: 1993, *Biosphere-Atmosphere Transfer Scheme (BATS) Version 1e as Coupled to the NCAR Community Climate Model*, National Center for Atmospheric Research, Boulder, CO, Tech Note/TN-387+STR, p. 80.
- Fearnside, P. M.: 1996, 'Amazonian Deforestation and Global Warming: Carbon Stocks in Vegetation Replacing Brazil's Amazon Forest', *Forest Ecol. Manage.* **80**, 21–34.
- Hahmann, A. N. and Dickinson, R.: 1997, 'RCCM2-BATS Model over Tropical South America: Application to Tropical Deforestation', *J. Climate* **10**, 1944–1964.
- Henderson-Sellers, A., Durbidge, T. B., Pitman, A. J., Dickinson, R. E., Kennedy, P. J., and McGuffie, K.: 1993, 'Tropical Deforestation: Modelling Local to Regional-Scale Climate Change', *J. Geophys. Res.* **98**, 7289–7315.
- Henderson-Sellers, A., McGuffie, K., and Gross, C.: 1995, 'Sensitivity of Global Climate Model Simulations to Increased Stomatal Resistance and CO₂ Increases', *J. Climate* **8**, 1001–1026.
- Houghton, J. T., Callander, B. A., and Varney, S. K.: 1992, *Climate Change 1992: The IPCC Supplementary Report to the IPCC Scientific Assessment*, Cambridge University Press, Cambridge, U.K., p. 121.
- Houghton, J. T., Jenkins, G. J., and Ephraums, J. J.: 1990, *Climate Change: The IPCC Scientific Assessment*, Cambridge University Press, Cambridge, U.K., p. 365.
- Houghton, J. T., Meira Filho, L. G., Callander, B. A., Harris, H., Kattenberg, A., and Maskell, K. (eds.): 1996, *The Science of Climate Change: Contribution of Working Group I to the Second Assessment of the Intergovernmental Panel on Climate Change*, Cambridge University Press, Cambridge, U.K., p. 572.
- Howe, W. and Henderson-Sellers, A. (eds.): 1997, *Assessing Climate Changes: The Story of the Model Evaluation Consortium for Climate Assessment*, Gordon and Breach Science Publishers, Sydney, p. 418.
- McGuffie, K., Henderson-Sellers, A., Zhang, H., Durbidge, T. B., and Pitman, A. J.: 1995, 'Global Climate Sensitivity to Tropical Deforestation', *Global Planet. Change* **10**, 97–128.
- Meehl, G. A. and Washington, W. M.: 1993, 'South Asian Summer Monsoon Variability in a Model with Doubled Atmospheric Carbon Dioxide Concentration', *Science* **260**, 1101–1103.
- Meehl, G. A. and Washington, W. M.: 1996, 'El Niño-Like Climate Change in a Model with Increased Atmospheric CO₂ Concentrations', *Nature* **382**, 56–60.
- Mylne, M. F. and Rowntree, P. R.: 1992, 'Modelling the Effects of Albedo Change Associated with Tropical Deforestation', *Clim. Change* **21**, 317–343.
- Pielke, R. A., Avissar, R., Raupach, M., Dolman, H., Zeng, X., and Denning, S.: 1998, 'Interactions between the Atmosphere and Terrestrial Ecosystems: Influence on Weather and Climate', *Global Change Biol.* **4**, 461–475.

- Pitman, A. J., Durbidge, T. B., Henderson-Sellers, A., and McGuffie, K.: 1993, 'Assessing Climate Model Sensitivity to Prescribed Deforestation Landscapes', *Int. J. Clim.* **13**, 879–898.
- Polcher, J. and Laval, K.: 1994, 'A Statistical Study of the Regional Impact of Deforestation on Climate in the LMD GCM', *Clim. Dyn.* **10**, 205–219.
- Sellers, P. J., Bounoua, L., Collatz, G. J., Randall, D. A., Dazlich, D. A., Los, S. O., Berry, J. A., Fung, I., Tucker, C. J., Field, C. B., and Jensen, T. G.: 1996, 'Comparison of Radiative and Physiological Effects of Doubled Atmospheric CO₂ on Climate', *Science* **271**, 1402–1406.
- Sellers, P. J., Dickinson, R. E., Randall, D. A., Betts, A. K., Hall, F. G., Berry, J. A., Collatz, G. J., Denning, A. S., Mooney, H. A., Nobre, C. A., Sato, N., Field, C. B., and Henderson-Sellers, A.: 1997, 'Modelling the Exchanges of Energy, Water, and Carbon between Continents and the Atmosphere', *Science* **275**, 502–509.
- Slingo, A.: 1989, 'A GCM Parameterization for the Shortwave Radiative Properties of Water Clouds', *J. Atmos. Sci.* **46**, 1419–1427.
- Sud, Y. C., Walker, G. K., Kim, J.-H., Liston, G. E., Sellers, P. J., and Lau, K.-M.: 1996, 'Biogeophysical Effects of a Tropical Deforestation Scenario: A GCM Simulation Study', *J. Climate* **9**, 3225–3247.
- Webster, P. J.: 1982, 'Seasonality in the Local and Remote Atmospheric Response to Sea Surface Temperature Anomalies', *J. Atmos. Sci.* **39**, 41–52.
- Zeng, N., Dickinson, R. E., and Zeng, X.: 1996, 'Climatic Impacts of Amazon Deforestation – A Mechanistic Model Study', *J. Climate* **9**, 859–883.
- Zhang, H., Henderson-Sellers, A., and McGuffie, K.: 1996a, 'Impacts of Tropical Deforestation I: Process Analysis of Local Climatic Change', *J. Climate* **9**, 1497–1517.
- Zhang, H., McGuffie, K., and Henderson-Sellers, A.: 1996b, 'Impacts of Tropical Deforestation II: The Role of Large-Scale Dynamics', *J. Climate* **9**, 2498–2521.

(Received 20 October 1999; in revised form 6 October 2000)